Restoration of *RUNX3* enhances transforming growth factor-β-dependent p21 expression in a biliary tract cancer cell line

Kazunori Hasegawa,[1] Shujiro Yazumi,[1] Manabu Wada,[1] Toshiharu Sakurai,[1] Masaya Kida,[1] Junichi Yamauchi,[1] Hiroshi Hisatsune,[1] Shinsuke Tada,[1] Hiroshi Ida,[1] Yuenn Nakase,[2] Chohei Sakakura,[2] Akeo Hagiwara[2] and Tsutomu Chiba[1,3]

[1]Department of Gastroenterology and Hepatology, Kyoto University Graduate School of Medicine, Kyoto, 606-8507; [2]Department of Digestive Surgery, Kyoto Prefectural University of Medicine, Kyoto, 602-8566, Japan

(Received September 24, 2006/Revised January 13, 2007/Accepted February 2, 2007/Online publication March 30, 2007)

***RUNX3* is a candidate tumor suppressor gene localized in 1p36, a region commonly inactivated by deletion and methylation in various human tumors. To elucidate the role of *RUNX3* in transforming growth factor (TGF)-β signaling in biliary tract cancer, we transfected Mz-ChA-2 cells, which do not express *RUNX3* but have intact TGF-β type II receptor and *SMAD4* genes, with the RUNX3 expression plasmid pcDNA3.1/RUNX3 or with the vector pcDNA3.1 as a control. Four Mz-ChA-2/*RUNX3* clones and one control clone were obtained. Although TGF-β1 only slightly inhibited growth of the control cells, growth inhibition and TGF-β-dependent G_1 arrest were significantly enhanced in the *RUNX3*-transfected clones. None of the clones, however, exhibited apoptosis. The slightly increased TGF-β1-induced p21 expression in the control clone was strongly enhanced in the *RUNX3*-transfected clones, and was accompanied by augmented decreases in the expression of cyclins D1 and E. When *RUNX3* small interfering RNA was added, TGF-β-dependent induction of p21 was reduced in the *RUNX3*-transfected clones. Xenografts of the clones in nude mice demonstrated that tumorigenicity was significantly decreased in the *RUNX3*-transfected clones in inverse proportion to the expression levels of RUNX3. Based on these results, *RUNX3* is involved in TGF-β-induced expression of p21 and the resulting induction of TGF-β-dependent G_1 arrest. (*Cancer Sci* 2007; 98: 838–843)**

Although carcinomas of the biliary tract are relatively rare, their incidence is increasing in Japan.[1] Most carcinomas of the biliary tract are unresectable when diagnosed, and their prognosis is poor because of high resistance to chemoradiation therapies.[2] Therefore, elucidating the biological characteristics of biliary tract cancer cells is necessary to establish better treatment strategies and thereby improve prognosis.

The *RUNX3* gene, which is located on chromosome 1 at 1p36.1, encodes a protein that belongs to the runt domain family of transcription factors that act as master regulators of gene expression in major developmental pathways.[3–5] Recent studies have revealed that *RUNX3* is frequently inactivated in various carcinomas, including gastric,[5] lung,[6,7] hepatocellular,[8] breast,[9] colon,[10] pancreatic and biliary tract,[11] prostate[12] and laryngeal carcinomas.[9] Interestingly, in primary cultures of *RUNX3*-null gastric epithelial cells, the cells are less sensitive to transforming growth factor (TGF)-β-dependent growth inhibition and apoptosis.[5] In addition, the RUNX3 protein has been found to bind the Smad2 and Smad3 proteins.[13] These data suggest a possible role for *RUNX3* in transducing TGF-β signaling.

TGF-β initiates its signal by bringing together type I and type II serine-threonine kinase receptors that form complexes with the ligand on the cell surface. This process results in the phosphorylation of the type I receptor by the type II receptor.[14] The type I receptor then phosphorylates and activates members of the Smad family of tumor suppressors (i.e. R-Smads), which includes Smad2 and Smad3.[14,15] The activated R-Smads form oligomers with the unique co-Smad, Smad4, and rapidly translocate to the nucleus to regulate expression of target genes. It is well known that TGF-β stimulation generally induces inhibition of cell growth, which involves various mechanisms, such as downregulation of c-myc and cyclin-dependent kinase (CDK)-2/CDK-4 activity by modulating the functions of $p15^{INK4B}$,[16,17] $p21^{Waf1/Cip1}$,[18,19] and/or $p27^{Kip1}$.[20,21] Among these factors, p21 plays a central role in the inhibition of CDK and in control of the cell cycle.

Forkhead transcription factor FOXO is a negative regulator of the PI3K/Akt pathway, which is activated by growth and survival cytokines such as insulin-like growth factor-1 and platelet-derived growth factor.[22] Among the FOXO family of molecules, FOXO3A directly binds and activates the p21 promoter, which has forkhead-binding elements adjacent to the SMAD-binding element, in cooperation with SMAD3 and SMAD4.[23] Moreover, Akt directly phosphorylates Smad3 to control TGF-β-dependent apoptosis or cell cycle arrest.[24] Altogether, the PI3K/Akt/FOXO pathway may have important cross-communication for TGF-β signaling.[25]

To elucidate the role of *RUNX3* in the TGF-β signaling pathway, we established and characterized stable transfectants of Mz-ChA-2 cells that constitutively expressed *RUNX3*. We demonstrate how the restoration of *RUNX3* expression in Mz-ChA-2 biliary tract cancer cells led to enhancement of TGF-β-induced upregulation of both p21 and FOXO3A and downregulation of cyclin D1 while significantly enhancing G_1 arrest. We also show how *RUNX3* is involved in the TGF-β-dependent expression of p21 and cell cycle arrest, most likely through upregulation of p21.

Materials and Methods

Cell lines, RUNX3 expression plasmid and small interfering RNA. The Mz-ChA-2 human biliary tract cancer cell line was a kind gift from Dr A. Knuth (Krankenhaus Nordwest, Frankfurt, Germany), and the human gastric cancer cell line MKN-1 was obtained from the American Type Culture Collection (Rockville, MD, USA). All cell lines were grown in MEM (Nikken Bio Medical Laboratory, Kyoto, Japan) supplemented with 10% fetal bovine serum (FBS) and antibiotics (100 IU/mL penicillin and 100 μg/mL streptomycin) in a water-saturated atmosphere of 5% CO_2.

The RUNX3 expression plasmid pcDNA3.1/RUNX3 was constructed by using full-length *RUNX3* cDNA as described previously.[26] To obtain stable transfectants, the Mz-ChA-2 cells were transfected with 5 μg pcDNA3.1/RUNX3 by using lipofectamine (Life Technologies, Rockville, MD, USA). At 24 h after transfection, the culture medium was replaced and supplemented

[3]To whom correspondence should be addressed. E-mail: chiba@kuhp.kyoto-u.ac.jp.

doi: 10.1111/j.1349-7006.2007.00460.x

with 400 μg/mL geneticin (G418 sulfate; Gibco BRL, Tokyo, Japan). The G418-resistant cells were grown in mass culture and cloned by limiting dilution in Dulbecco's modified Eagle's Medium (DMEM) containing 10% FBS and 200 mg/mL G418. Mz-ChA-2 cells that were stably transfected with pcDNA3.1 were used as a control.

To decrease the expression of RUNX3 and SMAD4, the Mz-Ch-A2 cells expressing RUNX3 were transfected with small interfering RNA (siRNA) fragment pairs that are homologous to human *RUNX3* and *SMAD4* (Amersham Biosciences, Piscataway, NJ, USA) by using TransIT TKO Transfection reagent (Mirus Bio Corporation, Madison, WI, USA).

RNA extraction and reverse transcription–polymerase chain reaction. Total cytoplasmic RNA was isolated by using TRIzol Reagent (Gibco BRL). For the reverse transcription–polymerase chain reaction (RT-PCR) procedure, cDNA was synthesized from 5 μg of total RNA by using an oligo-dT primer (Superscript kit; Gibco BRL) according to the manufacturer's manual. For human *RUNX3* transcripts, 5′-AGACGGCACCGGCAGAAG-3′ was used as a sense primer and 5′-TGTAGGGGAAGGCAGCTGAC-3′ as an antisense primer to amplify a region corresponding to 301 bp (nucleotides 541–841) of the human *RUNX3* sequence using the cDNA as a template. For the human *p15* transcripts, 5′-TCACAGGGGTTCCCTTCTCTC-3′ was used as a sense primer and 5′-CACTTCTTTGTGCCATCCATGG-3′ as an antisense primer to amplify a region corresponding to 500 bp (nucleotides 2405–2904) of the human *p15* sequence. The PCR were carried out in a thermal cycler (Perkin Elmer, Tokyo, Japan); the cDNA was denatured for 1 min at 94°C, then for 35 cycles of 30 s at 94°C, 30 s at 55°C, and 2 min at 72°C.

Real-time quantitative RT-PCR. Real-time RT-PCR amplification and data analysis were carried out using an ABI Prism 7700 Sequence Detector System (PE Applied Biosystems, Foster City, CA, USA) as described previously.[27] PCR primers and probes for FOXO3A (forward, 5′-CCCAGCCTAACCAGGGAAGT-3′; reverse, 5′-AGCGCCCTGGGTTTGG-3′; fluorogenic probe, 5′-TGACAACCCCAACCTGCCACCC-3′), and human 18S ribosomal RNA (forward, 5′-TAGAGTGTTCAAAGCAGGCCC-3′; reverse, 5′-CCAACAAAATAGAACCGCGGT-3′; fluorogenic probe, 5′-CGCCTAGATACCGCAGCTAGGAATAATG-3′) were designed by using the Primer Express program (PE Applied Biosystems).

Luciferase assay. To measure TGF-β signaling, the p3TP-Lux reporter plasmid (generous gift from Dr J. Massague, Howard Hughes Medical Institute, Memorial Sloan-Kettering Cancer Center, New York, NY, USA) containing the plasminogen activator inhibitor-1 promoter was used. Cells were seeded at a density of 3×10^5/well in six-well plates for 24 h, then transiently transfected with 0.1 μg p3TP-Lux reporter plasmid and as an internal control 0.02 μg pRL-TK vector (Promega, Madison, WI, USA) using Lipofectamine 2000 according to manufacturer's instruction (Invitrogen, Carlsbad, CA, USA). At 24 h later, cells were treated with 5 ng/mL TGF-β1 in DMEM with 0.5% FBS for 6 h. The cell lysates were analyzed for luciferase activity using the Dual-Luciferase Reporter Assay System (Promega). Reporter activities are presented as means ± SD of at least three independent experiments.

Growth inhibition assay. As described previously,[28] growth inhibition was assessed photometrically by using a Cell Counting Kit-8 (Dojindo, Kumamoto, Japan). Briefly, 5×10^3 cells were seeded per well in 96-well culture plates and then incubated for 24 h at 37°C in an atmosphere of 5% CO_2. The medium was then changed to DMEM that contained 0.5% FBS in the presence or absence of 5 ng/mL recombinant human TGF-β1 (R&D Systems, Tokyo, Japan) with or without 10 μg/mL anti-TGF-β1 neutralizing antibody (R&D Systems). After incubating for 48 h, the plates were incubated for another 3 h in 100 μL serum-free medium to which 10 μL of the Cell Counting Kit-8 reagent had been added. The plates were read at an optical density of 450 nm in a spectrophotometer referenced at 620 nm (Multiskan MS; Dainippon, Osaka, Japan). The effects of TGF-β1 on cell growth were expressed as the percentage of cells not affected by TGF-β1. All experiments were repeated six times, and the representative data are shown.

Terminal deoxynucleotidyl transferase-meditated dUTP nick-end labeling assay. The Mz-ChA-2 clones expressing RUNX3 and the mock vector-transfected Mz-ChA-2 clone (control) were cultured in four-well culture slides (Falcon, Bedford, MA, USA) in DMEM that contained 0.5% FBS in the presence or absence of 5 ng/mL TGF-β1. Forty-eight hours later, the slides were rinsed with phosphate-buffered saline (PBS) and fixed with 10% buffered formalin for 30 min. The clones were then stained by using an In Situ Cell Death Detection Kit (Roche, Indianapolis, IN, USA) according to the manufacturer's protocol. The terminal deoxynucleotidyl transferase-meditated dUTP nick-end labeling (TUNEL) index was calculated as the percentage of positive cells within the same field of 100 cells.

Analysis of cell cycle phase distribution. To investigate the biological relationship between RUNX3 and cell cycle-associated proteins, *RUNX3*-restored Mz-ChA-2 clone 1, which expressed RUNX3 most strongly, and a control vector-transfected Mz-ChA-2 clone were cultured for 48 h in DMEM that contained 0.5% FBS in the presence or absence of 5 ng/mL TGF-β1. Cells were harvested with 4 mM ethylenediaminetetracetic acid (EDTA)/PBS, fixed in 70% ethanol, and stained with 5 μg/mL propidium iodide (PI; Sigma Aldrich, St Louis, MO, USA). The DNA content of the cells was analyzed with a flow cytometer (EPICS XL; Beckman Coulter, Tokyo, Japan).

Western blot analysis. Cells were washed twice with ice-cold PBS and lysed in 20 mM Tris-HCl buffer (pH 7.4) containing 150 mM NaCl, 2 mM EDTA, 1% Nonidet P-40, 50 mM NaF, 1 mM Na_3VO_4, 1 mM Na_2MoO_4, 10 μM aprotinin and 10 μM leupeptin. The solution was centrifuged at 12 500 *g* for 10 min, and the supernatant was removed. Equal amounts of cell lysate protein extracts were fractionated by sodium dodecyl sulfate–polyacrylamide gel electrophoresis and transferred to an Immobilin-P membrane (Millipore, Bedford, MA, USA). The membranes were incubated with anti-p21, anti-p27 (Transduction Laboratories, Newington, NH, USA), anticyclin E, anticyclin D1, antic-myc, anti-SMAD4 (Santa Cruz Biotech, Santa Cruz, CA, USA) and anti-RUNX3[29] antibodies for 12 h at 4°C, with β-actin antibodies for 1 h at 37°C, and then with peroxidase-conjugated secondary antibodies for 1 h at 37°C. The blotted proteins were detected by using an ECL kit (Amersham Pharmacia Biotech, Buckinghamshire, UK). The same experiments were carried out three times, and the representative data are shown.

Tumorigenicity in nude mice. Four-week-old male BALB/cAJcl-nu mice (Nippon Clea, Osaka, Japan) were injected subcutaneously with exponentially growing Mz-ChA-2 cells (1×10^7) transfected with either pcDNA3.1/RUNX3 or pcDNA3.1 in a total volume of 500 μL PBS. All mice were killed 3 months after being inoculated, and the existence of the tumor nodule was confirmed histopathologically.

This work was carried out under the Japanese Law Concerning the Care and Control of Animals and was approved by the Animal Research Committee at the Kyoto University Graduate School of Medicine.

Statistical analysis. All numerical data were expressed as means ± SD. Differences among the mean values were evaluated by using Student's *t*-test. *P*-values below 0.05 were considered to be statistically significant.

Results

Restoring RUNX3 expression in Mz-ChA-2 cells. To investigate the function of *RUNX3*, we chose human biliary tract cancer cell line Mz-ChA-2 because Mz-ChA-2 cells do not express *RUNX3*

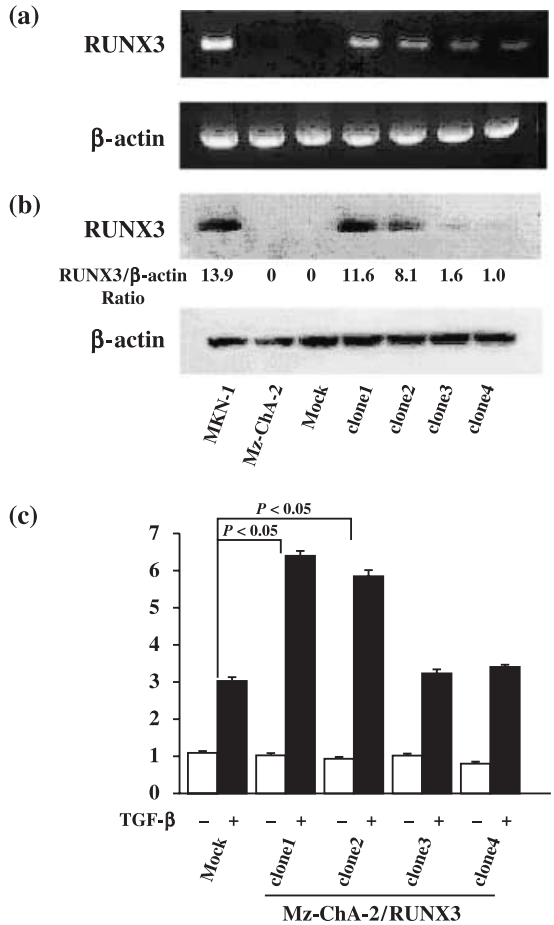

Fig. 1. *RUNX3* expression in a biliary tract cancer cell line Mz-ChA-2, mock vector-transfected Mz-ChA-2 cells (control), and the four *RUNX3*-restored Mz-ChA-2 clones. (a) *RUNX3* mRNA expression visualized by reverse transcription–polymerase chain reaction. (b) RUNX3 expression visualized by western blot analysis. Densitometric analysis revealed that the expression levels of RUNX3 in clones 1, 2 and 3 were, respectively, 11.6, 8.1 and 1.3 times greater than that in clone 4. The gastric cancer cell line MKN-1[39] was used as a positive RUNX3-expressing control. (c) Effect of transforming growth factor (TGF)-β1 on the luciferase activity of *RUNX3*-restored Mz-ChA-2 cells. Luciferase induction by TGF-β1 treatment was analyzed by using p3TP-Lux-transfected cells (3×10^5) incubated for 6 h with and without 5 ng/mL TGF-β1 in Dulbecco's modified Eagle's medium with 0.5% fetal bovine serum. The data are expressed as means ± SD of three independent experiments.

and have no alteration in other known molecules in the TGF-β-signaling pathway, such as the TGF-β type II receptor and *SMAD4* genes.[11,28] By introducing a RUNX3-expressing vector into Mz-ChA-2 cells, we obtained four Mz-ChA-2 clones that stably expressed *RUNX3* (Fig. 1a). Western blot analysis demonstrated that the expression levels of RUNX3 in clones 1, 2 and 3 were, respectively, 11.6, 8.1 and 1.3 times greater than that in clone 4 (Fig. 1b). However, untransfected and vector-transfected Mz-ChA-2 cells did not express *RUNX3* RNA or RUNX3 protein.

TGF-β1-induced growth suppression and luciferase assay. Adding TGF-β1 to the cell cultures inhibited growth of the Mz-ChA-2 cells transfected with the mock vector by 20% (±2.8%). TGF-β1 elicited a significantly greater inhibition of the growth of *RUNX3*-restored Mz-ChA-2 clones 1 and 2 than of mock vector-transfected cells (Table 1). Although TGF-β1 also inhibited the growth of clones 3 and 4, the inhibitory effects on these clones were not significantly different from those on the cells

Table 1. Effects of *RUNX3* restoration on transforming growth factor (TGF)-β1-induced growth inhibition of Mz-ChA-2 cells

Cell line	Anti-TGF-β antibody (–)	Anti-TGF-β antibody (+)
Mz-ChA-2 (mock)	20.0 ± 2.8	1.1 ± 3.2
Mz-ChA-2 (RUNX3)		
Clone 1	50.2 ± 8.1*	1.6 ± 3.3
Clone 2	35.0 ± 4.2*	0.0 ± 5.2
Clone 3	23.3 ± 4.6	0.7 ± 5.2
Clone 4	21.6 ± 3.6	2.9 ± 4.1

Cells (5×10^3) were incubated with or without TGF-β1 (5 ng/mL) in media containing 0.5% fetal bovine serum for 48 h. Values are expressed as the percentage of growth inhibition as determined by a comparison with the growth of non-stimulated cells (without TGF-β1; 100%). The data were calculated as the means ± SD of six experiments. *$P < 0.05$ when compared with the value derived by TGF-β1 stimulation in mock vector-transfected cells.

Table 2. Effects of *RUNX3* restoration on transforming growth factor (TGF)-β-induced apoptosis in Mz-ChA-2 cells

Cell line	TUNEL positive cells (%)	
	TGF-β1 (–)	TGF-β1 (+)
Mz-ChA-2 (mock)	7.2 ± 1.6	8.7 ± 1.4
Mz-ChA-2 (RUNX3)		
Clone 1	8.5 ± 1.7*	9.3 ± 2.3*
Clone 2	6.4 ± 1.4*	7.8 ± 1.0*
Clone 3	6.6 ± 2.1*	7.6 ± 0.8*
Clone 4	5.2 ± 0.7*	6.8 ± 1.9*

Mz-ChA-2 cells (5×10^3) were incubated with or without (control) TGF-β1 (5 ng/mL) in media containing 0.5% fetal bovine serum for 48 h and a terminal deoxynucleotidyl transferase-meditated dUTP nick-end labeling (TUNEL) assay was carried out. Values are expressed as the percentage of TUNEL-positive cells among 100 cells. The data were calculated as the means ± SD of five experiments. *Not significantly different from the value derived in the mock vector-transfected cells.

transfected with the mock vector. All of these growth-inhibitory effects of TGF-β1 were neutralized by adding 10 μg/mL of anti-TGF-β1 antibody to the culture medium. These results suggest that *RUNX3* is involved in TGF-β-induced growth inhibition.

The TGF-β1-mediated luciferase activity was elevated in all cells. TGF-β1 elicited significantly greater induction of luciferase assay in RUNX3-restored clones 1 and 2 than Mz-ChA-2 mock transfectant, but no significant inductions in RUNX3-restored clones 3 and 4 were observed (Fig. 1c). This result suggested that RUNX3 would enhance TGF-β signaling.

Apoptosis assay. We conducted a TUNEL analysis because previous reports demonstrated that restoration of *RUNX3* expression enhances TGF-β-dependent apoptosis.[5,29,30] In contrast to these previously published data, however, we did not observe TGF-β-induced apoptosis in either the mock vector-transfected clones or in any of the *RUNX3*-transfected Mz-ChA-2 clones (Table 2).

Cell cycle analysis. To investigate the role of *RUNX3* in the cell cycle, flow cytometry was used to examine the effects of TGF-β1 on the cell cycle of *RUNX3*-restored Mz-ChA-2 clone 1. Adding TGF-β1 to the cell culture caused a slight increase in the G_1 fraction, even in the mock vector-transfected Mz-ChA-2 cells (51.0 vs 68.5%). However, the TGF-β1-induced increase in the G_1 fraction in clone 1 was prominently enhanced when compared to the mock vector-transfected cells (54.2 vs 80.1%) (Fig. 2). Moreover, the percentage of cells that contained sub-G_1 DNA in both the mock vector-transfected Mz-ChA-2 clone and in *RUNX3*-restored Mz-ChA-2 clone 1 were less than 5%, irrespective of the presence of TGF-β1.

doi: 10.1111/j.1349-7006.2007.00460.x

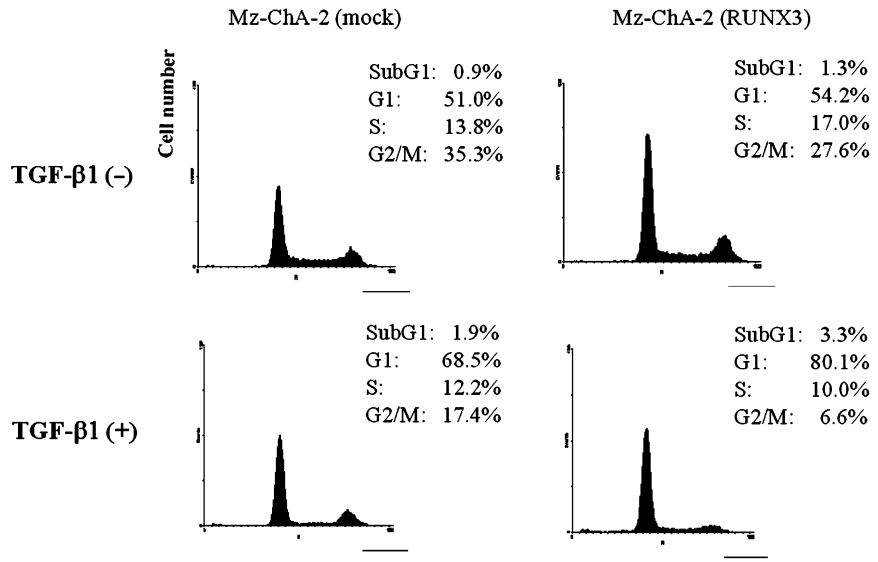

Fig. 2. Effects of *RUNX3* restoration on the cell cycle progression of Mz-ChA-2 cells after treatment with transforming growth factor (TGF)-β1. The histograms of vector-transfected Mz-ChA-2 cells (mock) or *RUNX3*-restored Mz-ChA-2 cells (clone 1) are shown 48 h after treatment with or without 5 ng/mL TGF-β1. The TGF-β1-induced increment of the G_1 fraction in clone 1 is prominently enhanced when compared to the mock vector-transfected cells. However, the percentage of cells with sub-G_1 DNA content in both the mock vector-transfected Mz-ChA-2 clone and in *RUNX3*-restored Mz-ChA-2 clone 1 are less than 5%, irrespective of the presence of TGF-β.

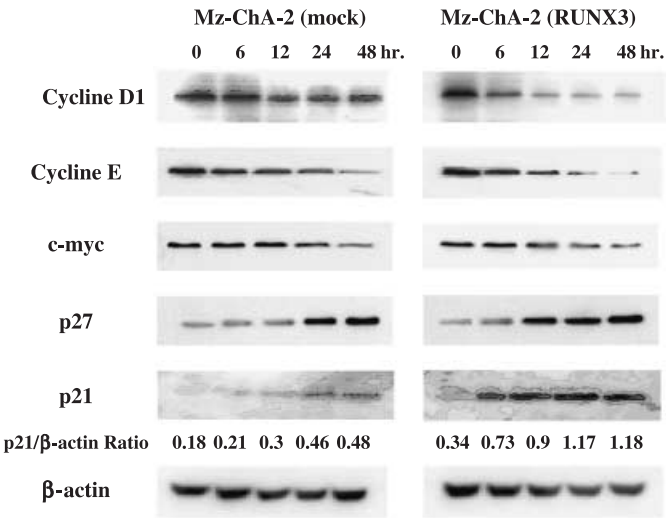

Fig. 3. Effects of *RUNX3* restoration on the expressions of various transforming growth factor (TGF)-β-dependent cell cycle-related proteins. Expressions of cell cycle-related proteins of vector-transfected Mz-ChA-2 cells (mock) or RUNX3-restored Mz-ChA-2 cells (clone 1) are shown 0, 6, 12, 24 and 48 h after treatment with 5 ng/mL TGF-β1. Densitometric ratios of p21 and β-actin are also shown.

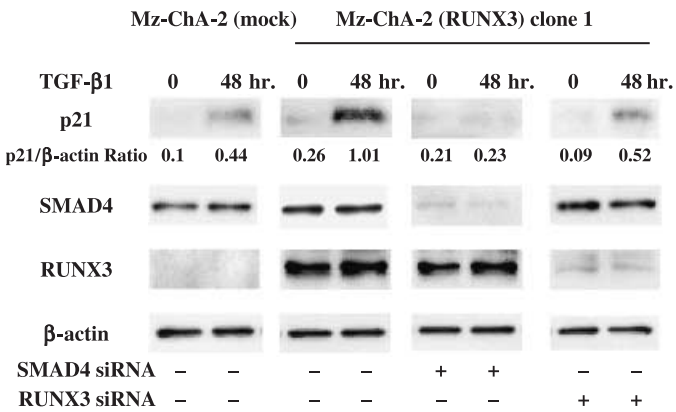

Fig. 4. Effects of RUNX3 or SMAD4 inhibition on transforming growth factor (TGF)-β1-dependent p21 expression in *RUNX3*-restored Mz-ChA-2 clone 1. Mock vector-transfected and *RUNX3*-restored Mz-ChA-2 cells were treated with 5 ng/mL TGF-β1 for 48 h. The TGF-β1-induced p21 expression is greatly reduced by adding not only *RUNX3* but also *SMAD4* small interfering RNA.

Expressions of cell cycle-associated proteins. To elucidate the mechanism by which TGF-β-induced G_1 cell cycle arrest is induced by *RUNX3* restoration, the expression of cell cycle-associated proteins was examined in mock vector-transfected Mz-ChA-2 cells and in *RUNX3*-restored clone 1. The expression of endogenous *p15* and the induction of p15 by TGF-β1 in Mz-ChA-2 cells were not confirmed, respectively, by RT-PCR and western blot analysis (data not shown). When compared to the control cells, the time-dependent decrease in the expression of cyclins D1 and E by TGF-β1 were both augmented in *RUNX3*-restored Mz-ChA-2 clone 1 (Fig. 3). However, the increased expression of p21 by TGF-β1 was clearly enhanced in clone 1 when compared to the mock vector-transfected cells (Fig. 3). In contrast, the TGF-β1-induced decrease in the expression of c-myc and the increase in the expression of p27 were not affected by the restoration of *RUNX3* (Fig. 3).

To confirm that restored *RUNX3* expression is involved in TGF-β1-induced p21 expression, the effects of *RUNX3* and *SMAD4* siRNA were examined in *RUNX3*-restored Mz-ChA-2 cells. Adding *RUNX3* and *SMAD4* siRNA almost completely abolished the expression of RUNX3 and SMAD4, respectively, in *RUNX3*-restored Mz-ChA-2 cells. The TGF-β1-induced expression of p21 was greatly reduced by adding both *RUNX3* and *SMAD4* siRNA (Fig. 4).

Expression of FOXO3A. The PI3K/Akt/FOXO pathway has been shown to greatly influence TGF-β signaling,[25] and the binding of FOXO3A to SMAD3 and SMAD4 is known to be required for the induction of p21 by TGF-β.[23] In examining whether TGF-β stimulation affects *FOXO3A* induction and whether *RUNX3* is involved in the expression of *FOXO3A*, we found that TGF-β1 stimulation increased *FOXO3A* mRNA expression even in the *RUNX3*-deficient Mz-ChA-2 cells (control). However, the TGF-β1-induced increase in *FOXO3A* expression was significantly enhanced in clone 1, which had the highest level of *RUNX3* expression. Moreover, the level of *FOXO3A* mRNA expression was proportional to the level of *RUNX3* expression in the *RUNX3*-restored clones (Fig. 5).

Tumorigenicity of RUNX3-restored Mz-ChA-2 clones in nude mice. Tumors formed in 8 of 10 BALB/cAJcl-nu mice that had been injected subcutaneously with mock vector-transfected Mz-ChA-2

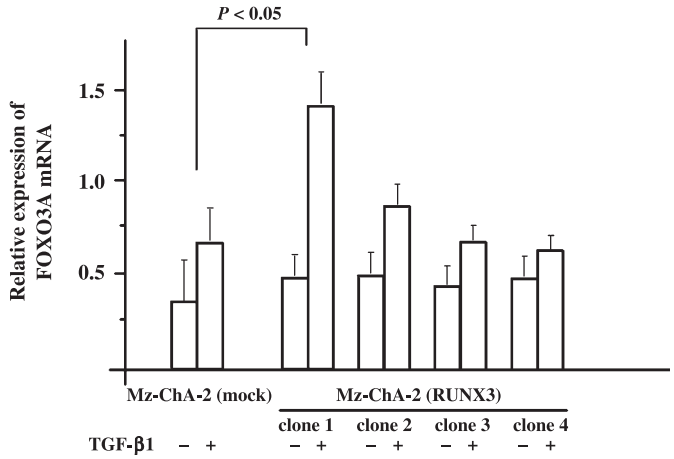

Fig. 5. Transforming growth factor (TGF)-β1-dependent *FOXO3A* mRNA expression in *RUNX3*-restored Mz-ChA-2 cells. *FOXO3A* mRNA expression was analyzed by real-time quantitative reverse transcription–polymerase chain reaction 48 h after treatment with or without 5 ng/mL TGF-β1. The data are expressed as means ± SD of three independent experiments. The increment of *FOXO3A* mRNA expression is proportional to the expression levels of RUNX3 in the *RUNX3*-restored clones. In particular, the increment of *FOXO3A* induction in clone 1 is significantly greater than that of the mock vector-transfected Mz-ChA-2 cells ($P < 0.05$).

Table 3. Tumor formation of *RUNX3*-expressing Mz-ChA-2 cells in nude mice

Cell line	Tumor formation
Mz-ChA-2 (mock)	8/10
Mz-ChA-2 (RUNX3)	
Clone 1	0/10*
Clone 2	0/10*
Clone 3	2/10*
Clone 4	3/10*

Mock vector-transfected or *RUNX3*-restored Mz-ChA-2 cells (clones 1–4) were injected subcutaneously in the same quantity (1×10^7 cells) into 4-week-old BALB/cAJcl mice. Each Mz-ChA-2 cell line was injected into 10 mice, for a total of 50 mice. Values are expressed as the ratio of the number of mice that developed a tumor per the total number of mice. *$P < 0.05$ when compared with the value derived in the control cell line (mock).

cells. In contrast, the formation of tumors was significantly reduced in mice injected with *RUNX3*-restored cells (Table 3). As described in Fig. 1, an inverse relationship was observed between the expression levels of *RUNX3* in the injected cells and the frequency of tumor formation.

Discussion

RUNX3 has been implicated as a tumor suppressor gene.[5] The gastric epithelium of *Runx3* knockout mice exhibits reduced TGF-β-dependent apoptosis, as well as cell-growth inhibition, suggesting that *RUNX3* exerts its tumor suppressor activity in a region downstream of the TGF-β signaling pathway.[26,31] Although previous studies demonstrated that overexpression of *RUNX3* enhanced TGF-β-dependent cell cycle arrest and apoptosis,[5,29,30,32] the precise role of *RUNX3* in the TGF-β signaling pathway remains unknown. In our study, we demonstrated that restoration of *RUNX3* in the Mz-ChA-2 cells significantly enhanced TGF-β-induced cell growth inhibition and TGF-β signaling. Furthermore, our study also showed that tumorigenicity of the Mz-ChA-2 cells, when injected into nude mice, was reduced in proportion to the expression levels of *RUNX3*. These data strongly suggest that *RUNX3* plays an important role in inhibiting cellular growth by participating in the TGF-β signaling pathway.

Several previous studies using gastric cancer cell lines have revealed that restoration of *RUNX3* enhanced TGF-β-dependent apoptosis.[29,32–34] For example, Yamamura *et al*. demonstrated that *RUNX3* directly activates the promoter activity of *Bim*, one of the proapoptotic *Bcl* family proteins, to enhance TGF-β-dependent apoptosis.[34] In contrast to their findings, we showed that restoration of *RUNX3* in Mz-ChA-2 cells did not affect apoptosis but enhanced TGF-β-dependent G_1 arrest. The reason for the discrepancy between their results and ours is unexplained at present. Although TGF-β did not elicit apoptosis in Mz-ChA-2 cells, it did enhance G_1 arrest slightly, even in the *RUNX3*-deficient Mz-ChA-2 cells in our experiments. It is possible therefore that the TGF-β dependency of the apoptotic mechanism differs between the gastric cancer cell lines Yamamura *et al*. used and the biliary tract cancer cells we used, irrespective of the presence or absence of *RUNX3*. Another consideration is that the nuclei of Mz-ChA-2 cells stain strongly for p53 (data not shown), which suggests that the abnormal function of p53 is involved in the insensitivity of the Mz-ChA-2 cells to the apoptotic signal of TGF-β.

Our study suggested that the enhancement of TGF-β-induced G_1 arrest by the restoration of *RUNX3* expression would be associated with upregulation of p21 and downregulation of cyclins D1 and E. Our data are in accord with the recent report by Chi *et al*.,[35] which demonstrated that the restoration of *RUNX3* enhanced TGF-β-induced p21 expression by direct activation of the *p21* promoter by RUNX3 in cooperation with SMAD3 and SMAD4 in gastric cancer cell lines. Thus, it appears reasonable to consider that the enhancement of TGF-β-induced G_1 arrest we observed is at least due in part to the enhanced expression of p21 by restoration of *RUNX3*.

TGF-β is also known to enhance p27.[36] Our study reconfirmed this finding, even in the *RUNX3*-deficient Mz-ChA-2 cells. Although a recent report suggested that *RUNX3* restoration also enhanced TGF-β-induced upregulation of p27,[32] the TGF-β1-induced increase of p27 expression in Mz-ChA-2 cells in our study was not affected by *RUNX3* restoration. Moreover, changes in c-myc expression have also been shown to be involved in TGF-β-dependent cell cycle regulation.[37,38] In our study, TGF-β elicited a slight decrease in c-myc expression in *RUNX3*-deficient Mz-ChA-2 cells. Similar to p27 expression, however, *RUNX3* restoration did not influence TGF-β-induced decrease of c-myc expression. Thus, in our study, TGF-β1-induced increase of p27 expression and decrease of c-myc expression were not affected, but increase of p21 expression was strongly enhanced by restoration of *RUNX3*. Although the reasons why p27 as well as c-myc expression were not affected by restoration of *RUNX3* in this study remains unknown, it is possible that *RUNX3* has different roles in TGF-β-dependent p21 and p27 as well as c-myc expressions. It may be noted that TGF-β-dependent cell cycle arrest is observed in association with p21 and p27 increase and c-myc decrease even in *RUNX3*-deficient Mz-Ch-A2 cells in our study. Thus, it is likely that *RUNX3* is not indispensable for TGF-β signaling, but is required for the potent inhibitory action of TGF-β on cell cycle arrest via enhancement of p21 expression.

Seoane *et al*. have shown that FOXO3A, a forkhead transcription factor, plays key roles in the TGF-β-dependent activation of p21 by partnering with Smad3 and Smad4.[23] It is noteworthy therefore that the induction of *FOXO3A* mRNA by TGF-β1 was enhanced in our study in proportion to the expression levels of RUNX3 in the *RUNX3*-restored Mz-ChA-2 clones. Because the *FOXO3A* promoter region has one complete *RUNX*-binding sequence (data not shown), it is reasonable to consider that *RUNX3* might directly control the expression of *FOXO3A* and that it affects TGF-β-induced p21 expression through this control mechanism.

doi: 10.1111/j.1349-7006.2007.00460.x

Clearly, the importance of cross-communication between TGF-β signaling and the PI3K/Akt/FOXO pathway is suggested.

Interestingly, even in *RUNX3*-restored clones 3 and 4, in which induction of *FOXO3A* by TGF-β1 as well as expression levels of RUNX3 are low, tumorigenicity were significantly reduced. The reason why tumorigenicity is reduced in clones with low induction of *FOXO3A* and low expression of RUNX3 in this study remains unknown. However, the tumor suppressor function of RUNX3 appears to be strongly enhanced *in vivo*. This result is in accord with the recent report by Sakakura *et al*., which demonstrated that RUNX3-transfected gastric cancer cells could not make metastatic lesions in nude mice although there were no significant differences between growth of RUNX3-restored clones and mock-transfected gastric cancer cells *in vitro*.[29]

In summary, our data showed that *RUNX3* plays important roles in TGF-β-induced p21 expression and cell cycle G_1 arrest in human biliary cancer cell line Mz-ChA-2. Further elucidation of the role of *RUNX3* as a tumor suppressor gene may contribute to the development of more optimal treatments for biliary tract carcinomas.

Acknowledgments

We thank Ms Pamela Paradis Tice, ELS(D), for editing the manuscript. This work was supported by a Grant-in-Aid for Scientific Research from the Ministries of Culture and Science and from the Ministry of Health, Labour and Welfare of Japan (grant numbers 16590591, 15209024, 16017249 and 17013051).

References

1 Shaib Y, El-Serag HB. The epidemiology of cholangiocarcinoma. *Semin Liver Dis* 2004; **24**: 115–25.
2 de Groen PC, Gores GJ, LaRusso NF, Gunderson LL, Nagorney DM. Biliary tract cancers. *N Engl J Med* 1999; **341**: 1368–78.
3 Ito Y. Molecular basis of tissue-specific gene expression mediated by the runt domain transcription factor PEBP2/CBF. *Genes Cells* 1999; **4**: 685–96.
4 Levanon D, Bernstein Y, Negreanu V *et al*. A large variety of alternatively spliced and differentially expressed mRNAs are encoded by the human acute myeloid leukemia gene AML1. *DNA Cell Biol* 1996; **15**: 175–85.
5 Li QL, Ito K, Sakakura C *et al*. Causal relationship between the loss of RUNX3 expression and gastric cancer. *Cell* 2002; **109**: 113–24.
6 Li QL, Kim HR, Kim WJ *et al*. Transcriptional silencing of the RUNX3 gene by CpG hypermethylation is associated with lung cancer. *Biochem Biophys Res Commun* 2004; **314**: 223–8.
7 Yanagawa N, Tamura G, Oizumi H, Takahashi N, Shimazaki Y, Motoyama T. Promoter hypermethylation of tumor suppressor and tumor-related genes in non-small cell lung cancers. *Cancer Sci* 2003; **94**: 589–92.
8 Xiao WH, Liu WW. Hemizygous deletion and hypermethylation of RUNX3 gene in hepatocellular carcinoma. *World J Gastroenterol* 2004; **10**: 376–80.
9 Kim TY, Lee HJ, Hwang KS *et al*. Methylation of RUNX3 in various types of human cancers and premalignant stages of gastric carcinoma. *Lab Invest* 2004; **84**: 479–84.
10 Goel A, Arnold CN, Tassone P *et al*. Epigenetic inactivation of RUNX3 in microsatellite unstable sporadic colon cancers. *Int J Cancer* 2004; **112**: 754–9.
11 Wada M, Yazumi S, Takaishi S *et al*. Frequent loss of *RUNX3* gene expression in human bile duct and pancreatic cancer cell lines. *Oncogene* 2004; **23**: 2401–7.
12 Kang GH, Lee S, Lee HJ, Hwang KS. Aberrant CpG island hypermethylation of multiple genes in prostate cancer and prostatic intraepithelial neoplasia. *J Pathol* 2004; **202**: 233–40.
13 Hanai J, Chen LF, Kanno T *et al*. Interaction and functional cooperation of PEBP2/CBF with Smads. Synergistic induction of the immunoglobulin germline Cα promoter. *J Biol Chem* 1999; **274**: 31 577–82.
14 Heldin CH, Miyazono K, ten Dijke P. TGF-β signalling from cell membrane to nucleus through SMAD proteins. *Nature* 1997; **390**: 465–71.
15 Massague J. How cells read TGF-β signals. *Nat Rev Mol Cell Biol* 2000; **1**: 169–78.
16 Li JM, Nichols MA, Chandrasekharan S, Xiong Y, Wang XF. Transforming growth factor beta activates the promoter of cyclin-dependent kinase inhibitor p15INK4B through an Sp1 consensus site. *J Biol Chem* 1995; **270**: 26 750–3.
17 Sandhu C, Garbe J, Bhattacharya N *et al*. Transforming growth factor beta stabilizes p15INK4B protein, increases p15INK4B–cdk4 complexes, and inhibits cyclin D1–cdk4 association in human mammary epithelial cells. *Mol Cell Biol* 1997; **17**: 2458–67.
18 Ducos K, Panterne B, Fortunel N, Hatzfeld A, Monier MN, Hatzfeld J. p21 (cip1) mRNA is controlled by endogenous transforming growth factor-β1 in quiescent human hematopoietic stem/progenitor cells. *J Cell Physiol* 2000; **184**: 80–5.
19 Miyazaki M, Ohashi R, Tsuji T, Mihara K, Gohda E, Namba M. Transforming growth factor-β1 stimulates or inhibits cell growth via down- or up-regulation of p21/Waf1. *Biochem Biophys Res Commun* 1998; **246**: 873–80.
20 Florenes VA, Bhattacharya N, Bani MR, Ben-David Y, Kerbel RS, Slingerland JM. TGF-β mediated G1 arrest in a human melanoma cell line lacking p15INK4B: evidence for cooperation between p21Cip1/WAF1 and p27Kip1. *Oncogene* 1996; **13**: 2447–57.
21 Tadlock L, Yamagiwa Y, Hawker J, Marienfeld C, Patel T. Transforming growth factor-beta inhibition of proteasomal activity: a potential mechanism of growth arrest. *Am J Physiol Cell Physiol* 2003; **285**: C277–85.
22 Vivanco I, Sawyers CL. The phosphatidylinositol 3-kinase AKT pathway in human cancer. *Nat Rev Cancer* 2002; **2**: 489–501.
23 Seoane J, Le HV, Shen L, Anderson SA, Massague J. Integration of Smad and forkhead pathways in the control of neuroepithelial and glioblastoma cell proliferation. *Cell* 2004; **117**: 211–23.
24 Conery AR, Cao Y, Thompson EA, Townsend CM Jr, Ko TC, Luo K. Akt interacts directly with Smad3 to regulate the sensitivity to TGF-β induced apoptosis. *Nat Cell Biol* 2004; **6**: 366–72.
25 Massague J, Seoane J, Wotton D. Smad transcription factors. *Genes Dev* 2005; **19**: 2783–810.
26 Ito K, Liu Q, Salto-Tellez M *et al*. RUNX3, a novel tumor suppressor, is frequently inactivated in gastric cancer by protein mislocalization. *Cancer Res* 2005; **65**: 7743–50.
27 Iwai A, Marusawa H, Kiuchi T *et al*. Role of a novel oncogenic protein, gankyrin, in hepatocyte proliferation. *J Gastroenterol* 2003; **38**: 751–8.
28 Yazumi S, Ko K, Watanabe N *et al*. Disrupted transforming growth factor-β signaling and deregulated growth in human biliary tract cancer cells. *Int J Cancer* 2000; **86**: 782–9.
29 Sakakura C, Hasegawa K, Miyagawa K *et al*. Possible involvement of RUNX3 silencing in the peritoneal metastases of gastric cancers. *Clin Cancer Res* 2005; **11**: 6479–88.
30 Torquati A, O'Rear L, Longobardi L, Spagnoli A, Richards WO, Daniel BR. RUNX3 inhibits cell proliferation and induces apoptosis by reinstating transforming growth factor beta responsiveness in esophageal adenocarcinoma cells. *Surgery* 2004; **136**: 310–16.
31 Fukamachi H, Ito K. Growth regulation of gastric epithelial cells by Runx3. *Oncogene* 2004; **23**: 4330–5.
32 Wei D, Gong W, Oh SC *et al*. Loss of RUNX3 expression significantly affects the clinical outcome of gastric cancer patients and its restoration causes drastic suppression of tumor growth and metastasis. *Cancer Res* 2005; **65**: 4809–16.
33 Ohgushi M, Kuroki S, Fukamachi H *et al*. Transforming growth factor beta-dependent sequential activation of Smad, Bim, and caspase-9 mediates physiological apoptosis in gastric epithelial cells. *Mol Cell Biol* 2005; **25**: 10 017–28.
34 Yamamura Y, Lee WL, Inoue KI *et al*. RUNX3 cooperates with FoxO3a to induce apoptosis in gastric cancer cells. *J Biol Chem* 2006; **281**: 5267–76.
35 Chi XZ, Yang JO, Lee KY *et al*. RUNX3 suppresses gastric epithelial cell growth by inducing p21 (WAF1/Cip1) expression in cooperation with transforming growth factor β-activated SMAD. *Mol Cell Biol* 2005; **25**: 8097–107.
36 Donovan JC, Rothenstein JM, Slingerland JM. Non-malignant and tumor-derived cells differ in their requirement for p27Kip1 in transforming growth factor-β-mediated G1 arrest. *J Biol Chem* 2002; **277**: 41 686–92.
37 Baldwin RL, Tran H, Karlan BY. Loss of c-myc repression coincides with ovarian cancer resistance to transforming growth factor beta growth arrest independent of transforming growth factor beta/Smad signaling. *Cancer Res* 2003; **63**: 1413–19.
38 Yagi K, Furuhashi M, Aoki H *et al*. c-myc is a downstream target of the Smad pathway. *J Biol Chem* 2002; **277**: 854–61.
39 Osaki M, Moriyama M, Adachi K *et al*. Expression of RUNX3 protein in human gastric mucosa, intestinal metaplasia and carcinoma. *Eur J Clin Invest* 2004; **34**: 605–12.